

Thin-Film Coalescence in Hydrogenated Amorphous Silicon Probed by Spectroscopic Ellipsometry with Millisecond-Scale Resolution

Y. M. Li,^{(1),(2)} Ilsin An,⁽¹⁾ H. V. Nguyen,⁽¹⁾ C. R. Wronski,⁽²⁾ and R. W. Collins⁽¹⁾

⁽¹⁾Materials Research Laboratory and Department of Physics, The Pennsylvania State University, University Park, Pennsylvania 16802

⁽²⁾Department of Electrical and Computer Engineering, The Pennsylvania State University, University Park, Pennsylvania 16802

(Received 24 June 1991; revised manuscript received 31 January 1992)

New developments in spectroscopic ellipsometry ($1.5 \leq h\nu \leq 4.3$ eV) now provide quantitative information on thin films with a time resolution of 16 ms. We report submonolayer sensitivity to a surface smoothing effect associated with nuclei coalescence in the early stages of hydrogenated amorphous silicon (*a*-Si:H) preparation by plasma-enhanced chemical vapor deposition. An investigation of *a*-Si:H prepared on *c*-Si and Cr substrates under different conditions of substrate temperature and plasma power discloses a clear correlation between the magnitude of this effect and the ultimate bulk properties of the material.

PACS numbers: 68.55.Jk, 07.60.Fs, 78.65.Gb, 81.15.-z

The morphological evolution of thin films is of great scientific and technological interest. To gain physical insights into thin-film phenomena, many authors have developed continuum models of film growth and studied the stability of evolving surface profiles in response to sinusoidal perturbations of wavelength, λ_r [1–5]. In models of ballistic deposition, for example, effects of finite atomic size [2] and shadowing [4] have been proposed to enhance these perturbations, whereas adatom surface diffusion damps them. Intuitively, one expects to regain a smooth profile for $\lambda_r < \lambda_0$, where λ_0 is the adatom surface diffusion length; however, when $\lambda_r > \lambda_0$, a strongly modulated profile ultimately develops that appears analogous to experimentally observed columnar microstructure [2].

The surface roughness associated with initial nucleation is a dominant perturbation for thin-film deposition on dissimilar substrates. One often strives to determine and/or control the evolution of surface morphology with subsequent growth because deposition processes leading to complete nuclei coalescence can avoid undesirable structural defects. A material of special interest in this regard is hydrogenated amorphous silicon (*a*-Si:H) owing to its extensive electronic applications. In fact for *a*-Si:H prepared by plasma-enhanced chemical vapor deposition (PECVD), a high film precursor diffusion coefficient, which drives surface smoothing in the continuum models, also enters into a specific model to explain the optimum conditions for electronic-grade material [6].

Noninvasive, real-time probes are needed to characterize such film-growth phenomena. Optical techniques such as ellipsometry are advantageous because they require no equipment *in vacuo*, and thus can be employed during PECVD [7]. Until our recent work [8,9], ellipsometry measurements have been confined to single or selected photon energies from the near infrared to the near ultraviolet, and the data are presented as trajectories in the parameters (ψ, Δ) (see below), swept out versus time during growth. For example, in one series of studies of *a*-Si:H PECVD on *c*-Si substrates, a lobe feature was

observed in the first 20–65 Å of the (ψ, Δ) trajectories, but only under growth conditions that led to electronic-grade material [10]. Although this feature was attributed to nucleation and the surface smoothing associated with nuclei coalescence, a quantitative comparison of depositions was not possible because of the complexity of the two-layer, thin-film optical model required to simulate the phenomenon.

With the development of real-time spectroscopic ellipsometry (SE), it is now possible to overcome such limitations, and even to validate the two-layer optical model for film growth. Of great importance is the recent improvement in time resolution: Continuous spectra can now be collected with monolayer sensitivity and millisecond-scale time resolution [11]. At this speed, the new technique of *time-resolved spectroscopic ellipsometry* is established, and here we describe its application to the important problem of nuclei coalescence in *a*-Si:H thin films.

A photodiode-array-based detection system is the unique feature of our rotating polarizer spectroscopic ellipsometer [8]. At a polarizer frequency of 31.3 Hz, a 48-point pair of (ψ, Δ) spectra from 1.5 to 4.3 eV can be acquired in one 16-ms optical cycle [11]. Here (ψ, Δ) are defined by $r_p/r_s \equiv \tan\psi \exp(i\Delta)$, where r_p and r_s are the complex reflection coefficients for *p*- and *s*-polarized light.

a-Si:H films were deposited by rf PECVD onto *c*-Si wafers covered either with native SiO₂ or smooth, opaque sputtered Cr. Both parallel-plate and remote He plasma configurations were used. The parameters leading to electronic-grade films for the former were as follows: 250°C substrate temperature (T_s), 20 standard cm³/min SiH₄ flow rate, 0.2 Torr pressure, and ~ 50 mW/cm² rf power flux at the sample surface. The corresponding parameters for the latter were 250°C, 5:50 SiH₄:He (in standard cm³/min), 0.4 Torr, and 300 mW/cm³ He plasma rf power density. A vacuum chamber, having ports oriented for optical access at a 70° incidence angle, was used for all depositions (base pressure, 10⁻⁸ Torr). In studies of the nuclei coalescence behavior, T_s and the rf power flux were varied.

The SE data-acquisition mode was tailored to the average deposition rates. For the standard (52 mW/cm²) and highest rf power (780 mW/cm²) parallel-plate PECVD *a*-Si:H, and for remote PECVD *a*-Si:H, the rates were ~ 80 , ~ 650 , and ~ 5 Å/min, respectively. For these depositions, the acquisition (repetition) times for full (ψ, Δ) spectra were 160 ms (1 s), 64 ms (64 ms), and 3.2 s (15 s), respectively. Thus, spectra were obtained as an average over 0.2–0.7-Å accumulation. With our fastest demonstrated acquisition (repetition) times of 16 ms (32 ms), 0.7-Å resolution can be achieved for a 2600-Å/min deposition rate [11].

For all PECVD films, we find that the two-layer optical model is a valid approximation to the structural evolution. Justification for this was provided by comparing the time dependence of the unbiased estimator of the mean-square deviation σ , a measure of the quality of the fit when the real-time (ψ, Δ) spectra are subjected to linear regression analyses, assuming film growth models having one, two, and more layers [12]. Throughout the thin-film nucleation and coalescence regimes, σ for the two-layer model is near our accuracy limits, and incorporation of additional layers does not lower σ any further. Three free microstructural parameters characterize the two-layer model: (1) d_s , the thickness of a surface layer of low bond-packing density; (2) d_b , the thickness of an underlying layer of bulk density; and (3) f_v , the surface layer bond-packing density (expressed as a void volume fraction). As demonstrated below, the surface layer simulates either the nuclei in the early growth stages or residual surface roughness after the first bulk monolayer forms.

The initial three steps in the interpretation of real-time SE data have been described earlier [9]. They involve determination of the dielectric function of the substrate components, then the substrate structure (e.g., native oxide thickness), and finally the dielectric function of the bulk layer of the deposited film. With this information, one can perform linear regression analysis since the two-layer model parameters to be determined, $\{d_s, d_b, f_v\}$, are photon-energy independent.

In these procedures, we make two assumptions: (1) that the bulk layer optical functions are independent of d_b and (2) that the surface layer optical functions are obtained from those of the bulk layer and f_v through the Bruggeman effective medium approximation [12]. Because size effects appear to be small for materials lacking long-range order, assumption (1) appears to be valid [13]. The problem with assumption (2), however, is that a larger fraction of Si atoms in the *a*-Si:H surface layer are bonded as $\text{Si}_{4-n}\text{H}_n$, $1 \leq n \leq 3$ [14]. In fact, for *a*-Si:H on Cr, inversion of (ψ, Δ) to obtain the dielectric function (ϵ_1, ϵ_2) is possible for 10–20-Å-thick nuclei. The results are typical of films containing more significant hydride bonding since the ϵ_2 maximum is blueshifted to 4 eV [15]. When this improved dielectric function is used

for the surface layer in the two-layer model, $\sigma(t)$ is improved but $d_s(t)$ and $d_b(t)$ are unaffected.

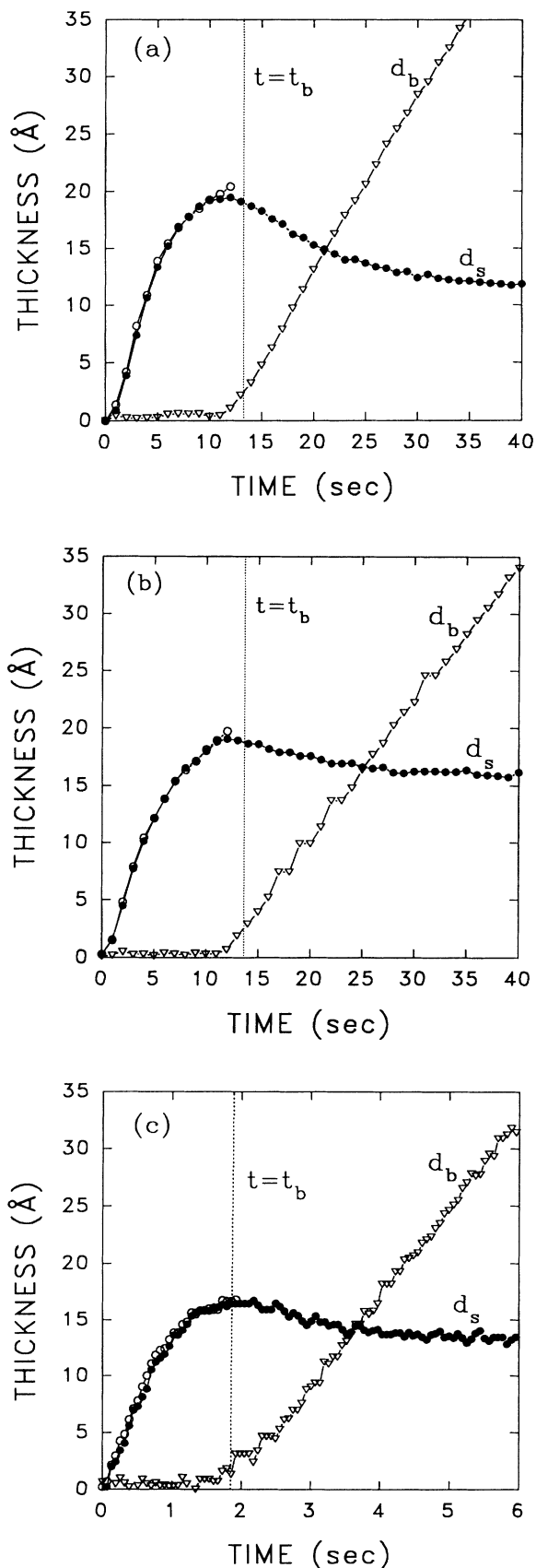
Results for the evolution of d_s and d_b in the two-layer model are given in Figs. 1(a)–1(c) for parallel-plate PECVD *a*-Si:H on native oxide-covered *c*-Si with (T_s , rf power) values of (250°C, 52 mW/cm²), (120°C, 52 mW/cm²), and (250°C, 520 mW/cm²), respectively. The open circles coinciding with d_s represent thicknesses deduced from the one-layer model in the nucleation regime prior to the formation of the first bulk monolayer (which occurs at time t_b , designated by the vertical lines at $d_b \sim 2.5$ Å). For times $t < t_b$, the difference between the one- and two-layer analyses is inconsequential since the submonolayer d_b values have little effect on the deduced value of d_s .

For $t < t_b$, the evolution of the bond-packing density, f_v , provides details on the nucleation geometry. The results for *a*-Si:H films on native-oxide covered *c*-Si and Cr suggest disk-shaped and hemispherical nuclei, respectively, consistent with earlier single-photon-energy studies [10]. For $t > t_b$, f_v stabilizes at ~ 0.5 in all cases; thus, this parameter is not of great interest here.

In this Letter, we will concentrate on the implications of Fig. 1 for the coalescence phenomenon. For $t \sim t_b$, the deposited flux begins contributing to the bulk layer which subsequently increases linearly with time. Thus, the onset of bulk film growth is also accompanied by a change in the behavior of d_s near $t \sim t_b$. *Once the first bulk monolayer forms, the evolution of d_s is a direct indication of the ability of subsequent flux to smooth nucleation-related surface morphology.* Thus, a connection is made to the stability analyses of film-growth models.

Surface layers for the three films of Fig. 1 prepared under standard conditions, at low T_s , and at high power, exhibit maxima of 19.5, 19, and 16.5 Å, and in the first 50 Å of bulk film growth, these values decay by 8, 3.5, and 3.5 Å, respectively [16]. The similarity of $d_s(t = t_b)$ in all cases indicates that the nucleation densities are similar. For example, if we were to assume that the disk-shaped nuclei form on a square lattice and evolve into hemispheres prior to contact [10], then nucleation densities of $(6\text{--}9) \times 10^{12} \text{ cm}^{-2}$ are obtained. With this geometry, the nuclei spacings (and thus the dominant λ_r values) range from 33 Å for high power *a*-Si:H to 39 Å for standard *a*-Si:H.

Although some differences among the *a*-Si:H depositions are small, trends observable in Fig. 1 are reproducible within $\sim \pm 0.5$ Å. The somewhat higher nucleation density for the high-power *a*-Si:H in comparison with the standard deposition shows that insufficient time is available at the higher deposition rate for surface diffusion and/or substrate defect passivation. The T_s -independent nucleation density, however, tends to suggest that the factor controlling the nucleation density is not surface diffusion but rather the density of defect sites on the *c*-Si



native oxide, since diffusion is expected to be strongly temperature dependent. A similar conclusion was reached based on our comparisons of pure *a*-Si deposition by sputtering onto native and thermal oxides of *c*-Si [9].

In fact in the latter studies, we found that for *a*-Si sputtered onto thermally oxidized *c*-Si, $d_s = 20$ Å at $t = t_b$, and this value *increases* with time by 12 Å in the first 25 Å of bulk film growth. This roughening of the *a*-Si surface in comparison to the smoothening observed in Fig. 1 for *a*-Si:H is easily understood. H passivation of the *a*-Si:H surface in PECVD lowers the kinetic mass transfer coefficient and, prior to incorporation at a reactive site, the precursors diffuse greater distances than atomic Si in sputtering. In order for optimum PECVD *a*-Si:H to smoothen, the precursor surface diffusion length λ_0 must satisfy $\lambda_0 > 40$ Å, whereas for the sputtered *a*-Si to roughen severely, $\lambda_0 \ll 40$ Å. The former result agrees with earlier studies that suggest $\lambda_0 \sim 60$ –100 Å for optimum PECVD *a*-Si:H, based on an analysis of substrate-induced roughness evolution during growth [10].

The differences in surface layer evolution in Fig. 1 also suggest trends in the surface diffusion length since the dominant post-nucleation λ_r is similar in all cases. The results for Figs. 1(b) and 1(c) suggest that for the lower T_s and higher plasma power, λ_0 has decreased, leading to a weakening of the coalescence phenomenon in both cases. The role of T_s in surface diffusion is obvious; however, the effect of plasma density is more complex. With a higher ionic flux, a greater number of reactive sites may be available where H has been removed from the *a*-Si:H surface [17,18]. In addition, the higher-power plasma may generate a higher concentration of SiH₂ and SiH radicals relative to SiH₃, and the former species are more reactive at the surface [18]. In either case λ_0 is expected to decrease, and this limits the healing of nucleation-induced structural heterogeneity.

Figure 2 shows the relaxation in d_s from its maximum in the first 50 Å of bulk film growth for a number of depositions on *c*-Si and Cr substrates, including results versus rf plasma power for parallel-plate PECVD *a*-Si:H and versus T_s for both parallel-plate and remote PECVD *a*-Si:H. The solid line depicts the trend for the parallel-plate PECVD samples on *c*-Si. The reduced smoothening effect evident in Fig. 2 for $T_s > 250$ °C may arise from the loss of surface H which increases the mass transfer

FIG. 1. Thicknesses of the surface layer (solid points) and bulk layer (triangles) deduced in an analysis of real-time SE data collected during the nucleation and growth of parallel-plate PECVD *a*-Si:H on native oxide-covered *c*-Si. Different conditions of substrate temperature and rf power were used: (a) 250°C and 52 mW/cm²; (b) 120°C and 52 mW/cm²; and (c) 250°C and 520 mW/cm². The open circles were obtained using a one-layer model in the regime where $\sigma(t)$ for the one- and two-layer models are equal.

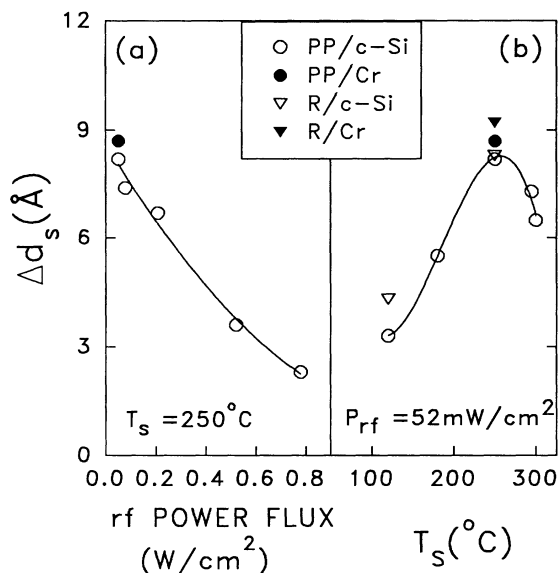


FIG. 2. Surface smoothing in the first 50 Å of bulk film growth for PECVD *a*-Si:H, plotted as a function of (a) rf plasma power at the sample surface and (b) substrate temperature. The key is as follows: PP, parallel-plate PECVD; R, remote He PECVD; Cr, sputtered chromium substrate; *c*-Si, native oxide-covered silicon wafer substrate. The solid lines are guides to the eye for the PP/*c*-Si depositions.

coefficient and likewise reduces surface diffusion [6].

Upon overall inspection of Fig. 2, it becomes obvious that the greatest surface smoothing in the parallel-plate configuration occurs under conditions commonly known to provide optimum electronic-grade *a*-Si:H, i.e., minimum plasma power and $T_s \sim 250^\circ C$. Thus, the conditions of lower precursor surface diffusion that lead to incomplete nuclei coalescence on the monolayer scale (and presumably a more defective surface microstructure) also give rise to the bulk defects that limit the electronic device quality of the *a*-Si:H. We propose that the smoothing phenomenon observed here is a manifestation of surface equilibration driven by diffusion that establishes a well-ordered Si network with a low density of defects (i.e., weak bonds and coordination defects).

In summary, we have developed spectroscopic ellipsometry with a resolution of 16 ms in order to characterize the nucleation and growth of thin films at high rates. We have applied this technique to study the early stages of PECVD of *a*-Si:H. SE provides submonolayer sensitivity to coalescence, i.e., the decay of nucleation-generated surface morphology, after nuclei make contact

to form the first bulk monolayer. We offer the first clear evidence of the dependence of precursor surface diffusion on substrate temperature and plasma power, thus identifying the important role it plays in determining the ultimate properties of the bulk material.

Funding was provided by the National Science Foundation under Grants No. DMR-8901031 and No. DMR-8957159, and the Solar Energy Research Institute under subcontract XG-1-10063-10. Two of us (Y.M.L. and C.R.W.) also acknowledge support from the Electric Power Research Institute.

- [1] C. H. J. van den Brekel and A. K. Jansen, *J. Cryst. Growth* **43**, 364 (1978).
- [2] A. Mazor, D. J. Srolovitz, P. S. Hagan, and B. G. Bukiet, *Phys. Rev. Lett.* **60**, 424 (1988).
- [3] G. S. Bales, A. C. Redfield, and A. Zangwill, *Phys. Rev. Lett.* **62**, 776 (1989).
- [4] R. P. U. Karunasiri, R. Bruinsma, and J. Rudnick, *Phys. Rev. Lett.* **62**, 788 (1989).
- [5] B. J. Palmer and R. G. Gordon, *Thin Solid Films* **177**, 141 (1989).
- [6] For a review see K. Tanaka and A. Matsuda, *Mater. Sci. Rep.* **2**, 139 (1987).
- [7] F. Hottier and J. B. Theeten, *J. Cryst. Growth* **48**, 644 (1980).
- [8] Y.-T. Kim, R. W. Collins, and K. Vedam, *Surf. Sci.* **223**, 341 (1990).
- [9] I. An, H. V. Nguyen, N. V. Nguyen, and R. W. Collins, *J. Vac. Sci. Technol. A* **9**, 622 (1991).
- [10] R. W. Collins and B.-Y. Yang, *J. Vac. Sci. Technol. B* **7**, 1155 (1989).
- [11] I. An, Y. M. Li, H. V. Nguyen, and R. W. Collins, *Rev. Sci. Instrum.* (to be published).
- [12] D. E. Aspnes, *Proc. Soc. Photo-Opt. Instrum. Eng.* **276**, 188 (1981).
- [13] R. W. Collins, I. An, H. V. Nguyen, and T. Gu, *Thin Solid Films* **206**, 374 (1991).
- [14] Y. Toyoshima, K. Arai, A. Matsuda, and K. Tanaka, *Appl. Phys. Lett.* **56**, 1540 (1990).
- [15] K. Mui and F. W. Smith, *Phys. Rev. B* **38**, 10623 (1988).
- [16] This smoothing effect continuing through the first 50 Å of bulk film growth gives rise to the lobe-cusp features observed in earlier single-photon-energy ellipsometry (ψ, Δ) trajectories [10].
- [17] C. C. Tsai, J. C. Knights, G. Chang, and B. Wacker, *J. Appl. Phys.* **59**, 2998 (1986).
- [18] A. Gallagher, in *Materials Issues in Amorphous-Semiconductor Technology*, edited by D. Adler, Y. Hamakawa, and A. Madan, MRS Symposia Proceedings No. 70 (Materials Research Society, Pittsburgh, 1986), p. 3.